Microsyst Technol (2012) 18:257–265
DOI 10.1007/s00542-011-1389-5

TECHNICAL PAPER

Hot embossing at viscous state to enhance filling process for complex polymer structures

Xuelin Zhu · Terrence W. Simon · Tianhong Cui

Received: 20 April 2011 / Accepted: 1 December 2011 / Published online: 17 December 2011
© Springer-Verlag 2011

Abstract In this paper, a new hot embossing process, molding at the viscous state, for fabrication of complex polymer structures at the micro and millimeter scale is presented. Polymer deformability is enhanced due to its low viscosity and is increased by an inner pressure from confinement of the polymer flow. Various millimeter-scale polymer structures with high aspect ratios and complex features were hot embossed. In addition, typical microstructures were achieved. This new approach promises the advantages of a broad process capability and strong compatibility with conventional hot embossing processes.

1 Introduction

Hot embossing has become a well established fabrication technique for polymer microstructures in last decades (Chou et al. 1995; Heckele et al. 1998; Guo 2004; Heckele and Schomburg 2004; Kumar et al. 2009). A wide variety of micro and nano polymer structures has been hot embossed for Microelectromechancial Systems, including actuators (Zhao and Cui 2003), optical devices (Choi 2004; Pan and Su 2007; Ting et al. 2008), and microfluidics (Zhu et al. 2006). The first issue for hot embossing is how to completely fill the mold insert cavity with polymer. This molding process is controlled by several process parameters, including molding temperature, force, and time. The required values of the process parameters are determined by the materials and the geometries of the embossed structures. For example, both amorphous and semicrystalline polymers are thermal plastics, but they have different molding temperature windows (Worgull et al. 2010). The molding temperature window for amorphous polymers is determined by the glass transition range (Worgull et al. 2010), while the molding temperature for a semicrystalline polymer is determined by the melting range. In previous research, thermal plastics were used mostly for hot embossing due to their wide molding temperature window from the elastic stage to the melting stage (Worgull et al. 2010). Molding of amorphous polymer structures is done with a wide range of process parameters. Normally the molding process is optimized on process parameters, including temperature, force, and time, by numerical simulations (Taylor et al. 2009) and experimental design (He et al. 2007). For most simple microstructures, the process window focuses on the elastic state (or the rubbery state) determined by the glass transition temperature (T_g). However, complex and large feature size structures are very difficult to directly mold with presently-used process parameters because the deformability of the rubber state polymer is insufficient to fill a mold cavity. Thus, further improvement beyond conventional hot embossing is needed to meet new demands. Several approaches were used to enhance the molding ability previously. For example, special designed tool was used to decrease the amount of lateral loss of polymer during molding process (Worgull 2009; Worgull et al. 2005). Complex embossing tool was also used to increase the internal pressure of molding polymer (Worgull 2009; Mehne et al. 2008; Dittrich 2004).

The strong relationship between mechanical strength and molding temperature for an amorphous polymer makes it possible for us to seek possible solutions. Change of

X. Zhu · T. W. Simon · T. Cui (✉)
Department of Mechanical Engineering,
University of Minnesota, 111 Church St,
Minneapolis, MN 55455, USA
e-mail: tcui@me.umn.edu

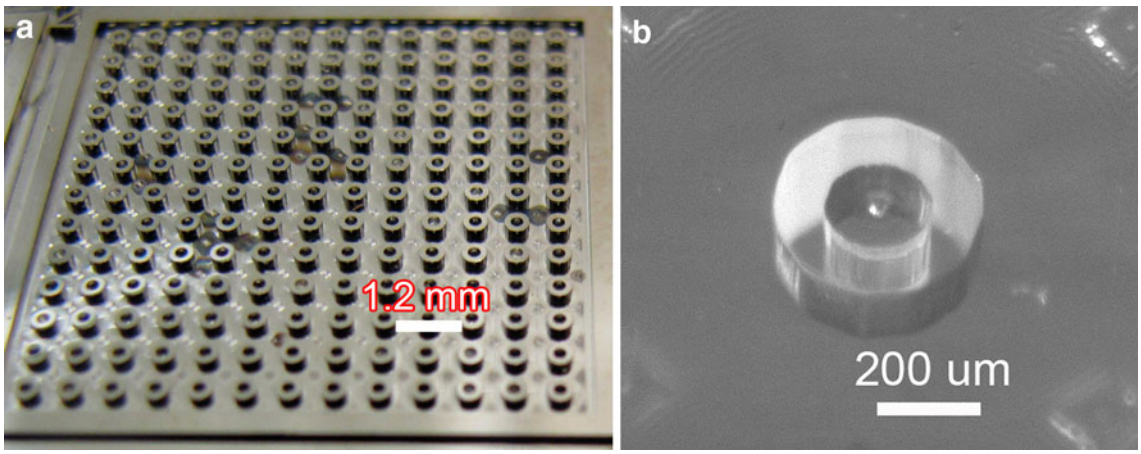

Fig. 1 Microstructures by hot embossing. **a** Nickel microneedle mold insert. **b** Hot embossed polymer (PMMA) a micro post in a micro well

polymers among different states when temperature changes must be considered. They act as rigid solids at temperature below T_g and turn into a rubbery state when the temperature rises higher than T_g. As the temperature rises further, they begin to flow. During these physical phase change processes, the mechanical strength drops quickly with increased temperature. For example, the Young's modulus of polymethyl methacrylate (PMMA) drops from 3 GPa to 0.1 MPa when temperature increases from room temperature to 160, 55°C higher than its T_g (Kumar et al. 2009; Worgull et al. 2006). Most simple PMMA microstructures can be molded at temperature close to T_g for most simple PMMA microstructures, the molding temperature is tens of degrees above T_g (Guo 2004; Heckele and Schomburg 2004). However, for hot embossing in the nano scales, higher molding temperature is desired to reduce polymer resistance to flow into a mold cavity. Early work adopted this method to replicate very high aspect ratios from LIGA mold insert (Roetting et al. 1999; Guo et al. 2007), and enable good PMMA flow ability in cavity (Shen et al. 2004). In these cases, for example, PMMA was molded at 75°C above T_g (Chou et al. 1995). In this case, PMMA behaves like a viscous flow.

Previous research indicates that molding in the viscous state has potential to widen process capabilities. A question remains of how to adopt the viscous state for the molding stage of a hot embossing process in a facile way. Basically, there are three issues. Firstly, the typical molding process parameters must be fixed, especially, the molding temperatures. Secondly, handling the polymer during the hot embossing process as it acts more like a viscous fluid than a rubber must be addressed. Thirdly, a possible need for improved mold inserts over convention molds must be considered.

Here, a new hot embossing process with molding at the viscous state is presented. Extensive process capability is achieved. Various complex or high-aspect-ratio structures at the micro and millimeter scales were successfully hot embossed. Compatibility with previous embossing processes is discussed.

2 Experimental methods

Our newly developed process is compatible with conventional hot embossing processes except we emboss at a different state of the polymer materials. Polymer materials are sandwiched by a mold insert and a hot plate, then heated to a viscous state. Molding force is applied to press the polymer to completely fill the mold cavity. Finally, the mold is detached from the polymer. Molding at viscous states requires improved mold designs.

2.1 Materials

Various polymers can be used in this fabrication process. Here, commercial PMMA is selected for demonstration because it has been routinely used in hot embossing processes. PMMA sheets 0.5 mm thick were baked at 80°C in an oven for 5 h before hot embossing begins.

2.2 Hot embossing machine

The hot embossing process is performed with a HEX01 (JENOPTIK, Germany) machine. There are two hot plates in this machine: a bottom stationary hot plate and a top movable hot plate. The maximum force and temperature are 50 kN and 320°C, respectively. A rotary pump is connected to an embossing chamber to provide a vacuum of lower than 0.1 mbar.

2.3 Mold designs and fabrication

Two types of molds were designed for demonstration: electroformed Nickel molds containing a micro-needle

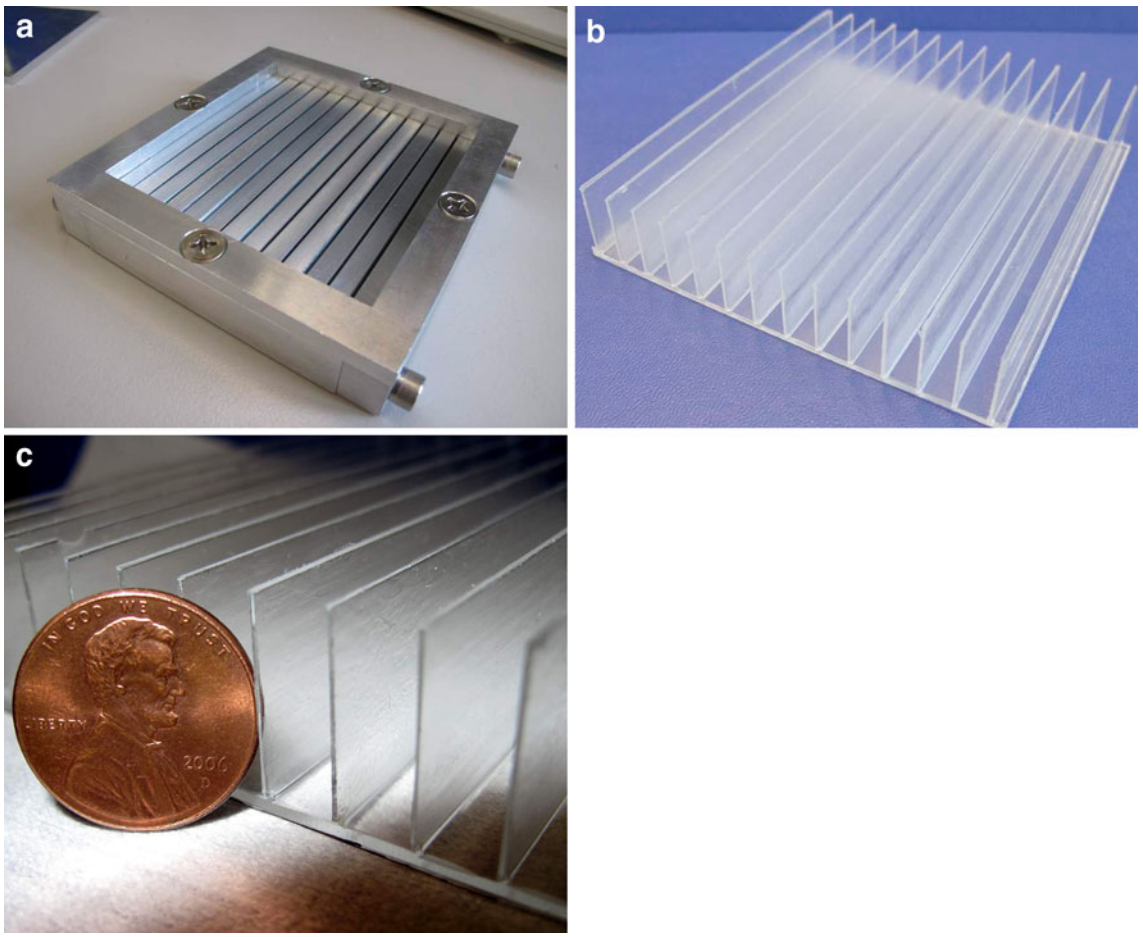

Fig. 2 Polymer agitators by hot embossing with an assembly mold insert. **a** Aluminum assembly mold insert. **b** Hot embossed agitators on a 10 cm × 10 cm area with a high aspect ratio of 35. The thickness and height of agitator are 0.5 and 17.5 mm respectively. **c** Zoom-in agitators compared with a US penny

arrays, and computer numerical control (CNC) machined stainless steel assembly molds with feature sizes at the millimeter scale. The micro needle is selected in this paper because of the enhanced filling process needs of the inner cavity. CNC molds require improved molding and demolding processes due to large feature sizes resulting in large molding and demolding forces.

2.3.1 *Micro scale nickel mold inserts through electroforming*

The nickel mold insert employed in this study is shown in Fig. 1a. The inner and outer diameters of the micro needles are 200 µm and 400 µm, respectively. The height is 250 µm. The mold was fabricated through UV lithography and electroforming processes, which are parts of the standard UV-LIGA process (Chang and Kim 2000; Zhu et al. 2006). Photoresist SU8 3050 (MicroChem, USA) was spin coated on 102 mm (4 inch) silicon wafers with Cr/Au (50/100 nm) seed layers, soft baked at 95°C for 1 h, and exposed to UV light at a dose of 350 mJ/cm^2 in a Karl Suss MA6 mask aligner (Karl Suss, Germany) using a printed mask (CAD Art Service, USA). Next, the mold was post baked at 95°C for 15 min, and developed in propylene glycol monomethyl ether acetate (Sigma-Aldrich, USA). The patterned SU8 photoresist was used as a mold for electroplating. A 3 mm thick layer of Nickel was then deposited using a direct current of 2.0 A in a SE101 (Digital Matrix, USA) plating station. The electroformed nickel mold insert was machined to adapt to the work holder in the hot embossing machine. Finally, the SU8 was removed using SU8 remover (MicroChem., USA).

2.3.2 *CNC machined metal mold insert with feature sizes at the millimeter scale*

Four metal mold inserts with a feature sizes in the millimeter scale were fabricated through a computer numerical control (CNC) machining process. Each mold insert had different structural features:

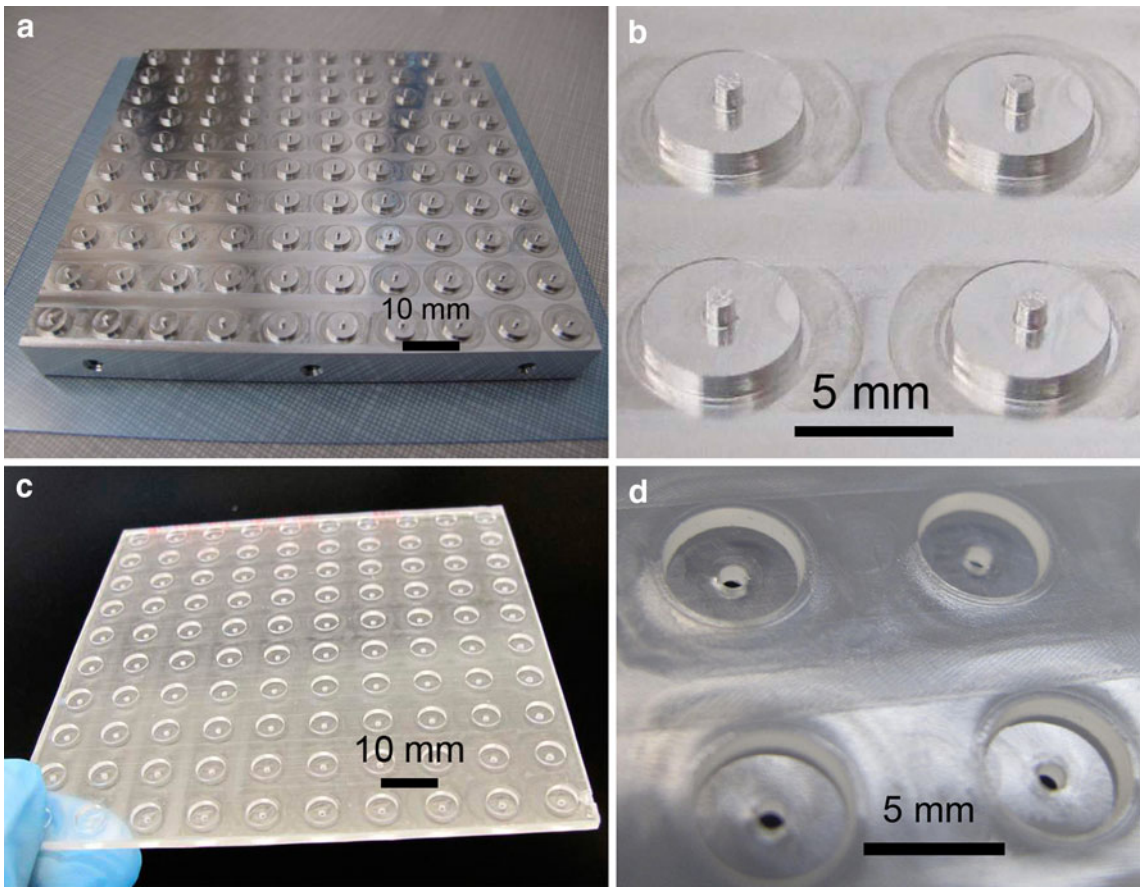

Fig. 3 Synthetic jet array by hot embossing with a monolithic mold. **a** CNC machined mold insert. **b** Zoom-in mold insert. **c** Hot embossed synthetic jet array on a 10 cm × 10 cm area, including cavities and nozzles. **d** Zoom-in synthetic jet

1. High-aspect-ratio agitators: This final polymer structure consists of 14 agitators of 0.5 mm thickness and 17.5 mm height on a 10 by 10 cm^2 plate. The aspect ratio reaches 35. Directly demolding of these high-aspect-ratio structures is very challenging. The absolute demolding force will be extremely large, even enough to destroy the hot-embossed structures. Thus, an assembly mold insert (shown in Fig. 2a) was designed for improved demolding. Metal bars were aligned and fixed by trenches on an outer frame. Each polymer agitator is defined by two metal bars. Disassembly of the components, one-by-one, promises a reduced demolding force.
2. Ten by ten synthetic jet array: this polymer structure consists of a 10 by 10 array of jets on a 10 × 10 cm^2 plate for a synthetic jet system. Each synthetic jet consists of a cavity and one or more nozzles. Each unit on the mold insert consists of two layer posts (Fig. 3a, b). The diameter of cavity and nozzle are 5.0 and 1.0 mm, respectively. Both are 1.0 mm deep. The CNC machined mold insert is designed as a monolithic structure instead of an assembly. One of reasons is that the total 100 synthetic jet array causes a low efficiency for assembly and disassembly. The demolding force is still a critical factor. A demolding angle of two degrees was chosen for the sidewalls of cavities to minimize demolding force.
3. Double-sided, high aspect ratio agitators: this configuration is designed to demonstrate double-sided hot embossing of millimeter scale polymer structures by an assembly mold insert. The final polymer structure consists of 26 agitators on each side of a plate. The thickness and height of agitators are 0.25 and 5.0 mm, respectively. The aspect ratio reaches 20. The plate area is 40 mm by 91 mm. The assembly mold insert is designed to decrease the demolding force. The mold consists of individual stainless steel bars with trenches on both sides (Fig. 4a). These metal bars are secured by screws (Fig. 4b). The polymer agitator is defined by the trenches, as shown in Fig. 4c. Polymer is sandwiched by the top and bottom molds, aligned by an outer frame.
4. Combination of agitators and synthetic jet array: this configuration is designed to demonstrate double-sided hot embossing of millimeter-scale complex polymer

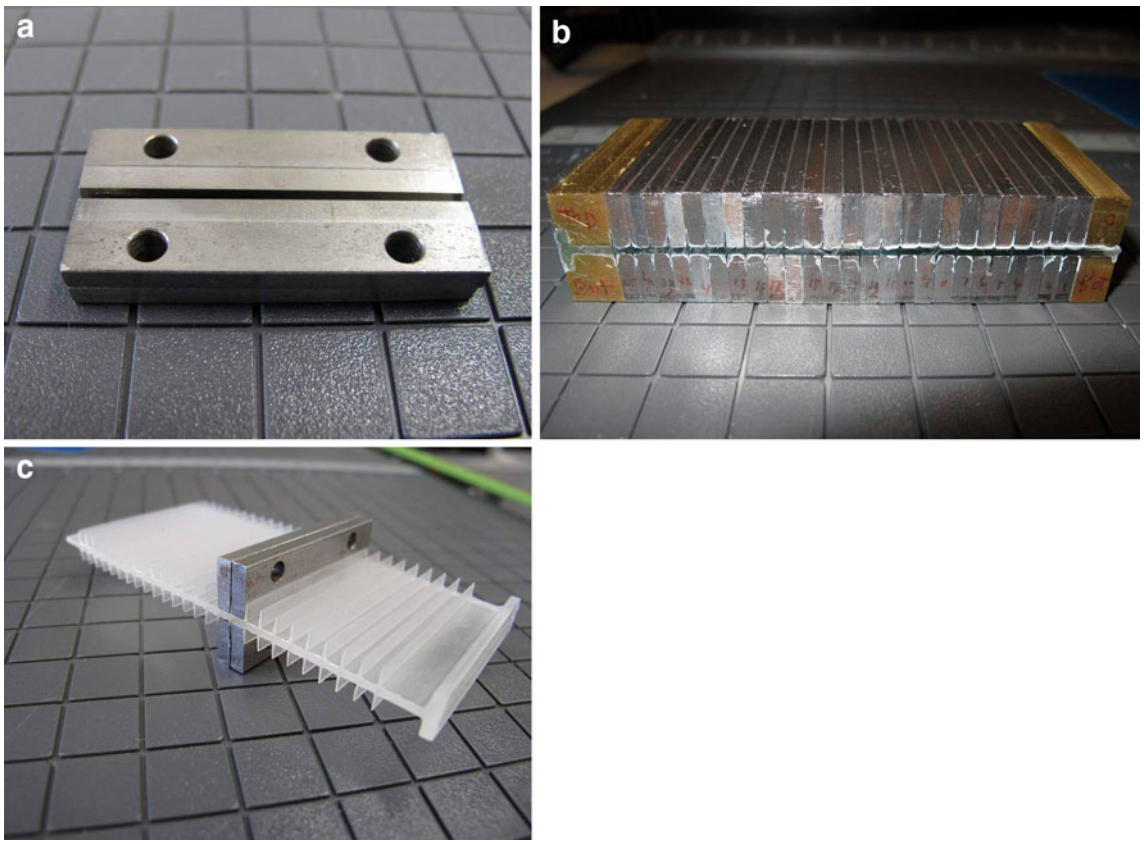

Fig. 4 Double-sided agitators made by a double-sided hot embossing process, with assembly mold inserts. **a** Metal bar with trenches on both sides. **b** Polymer agitators embedded in a mold insert before demolding. **c** Hot embossed, double-sided polymer agitators

structures by assembly and monolithic mold inserts, as shown in Fig. 5. The final polymer structures consist of agitators and a synthetic jet array on the top and bottom sides. The top mold consists of individual metal bars guided by trenches on an outer chamber. The thickness and height of an agitator are 1.0 and 7.0 mm, respectively. The bottom synthetic jet mold is the same as the previous synthetic jet mold.

2.4 Hot embossing process

The process in this work is compatible with micro hot embossing except some different parameters including temperature and time must be considered. The mold insert and polymer PMMA are heated up to 190, 85°C above the glass transition temperature of PMMA. A molding force of 20–30 kN on a 10 cm by 10 cm area is applied for a duration from 2 to 10 min. The molding force is released after the sample is cooled below 85°C. The mold insert is detached from the hot embossed polymer structures. The overall hot embossing parameters are shown in Table 1.

3 Results and discussion

3.1 Results

Several typical polymer structures were hot embossed with features including high aspect ratios and multiple layers. Figure 1 shows a hot embossed microstructure consisting of a polymer post in a polymer well. The post molding is always slower than the well molding due to the larger flow resistance. Experiments show that it is hard to get fully replicated posts by hot embossing when in the rubbery state. In our hot embossed sample, the top surface of the micro posts and wells are at the same level. The corner of the post is as sharp as that of mold insert. These features indicate that the micro post was fully replicated from the mold insert. Figure 2 shows the hot embossed agitators on a 10 cm × 10 cm area. All these completely replicated agitators show no bending. This indicates that the residual internal stresses are very low. This is a result of our new process. Polymer is pressed into the mold insert cavity and redistributes until it reaches a steady state. Figure 3 shows the hot embossed 10 by 10 synthetic jet array on a 10 cm by 10 cm area. More than 90% of the volume of the

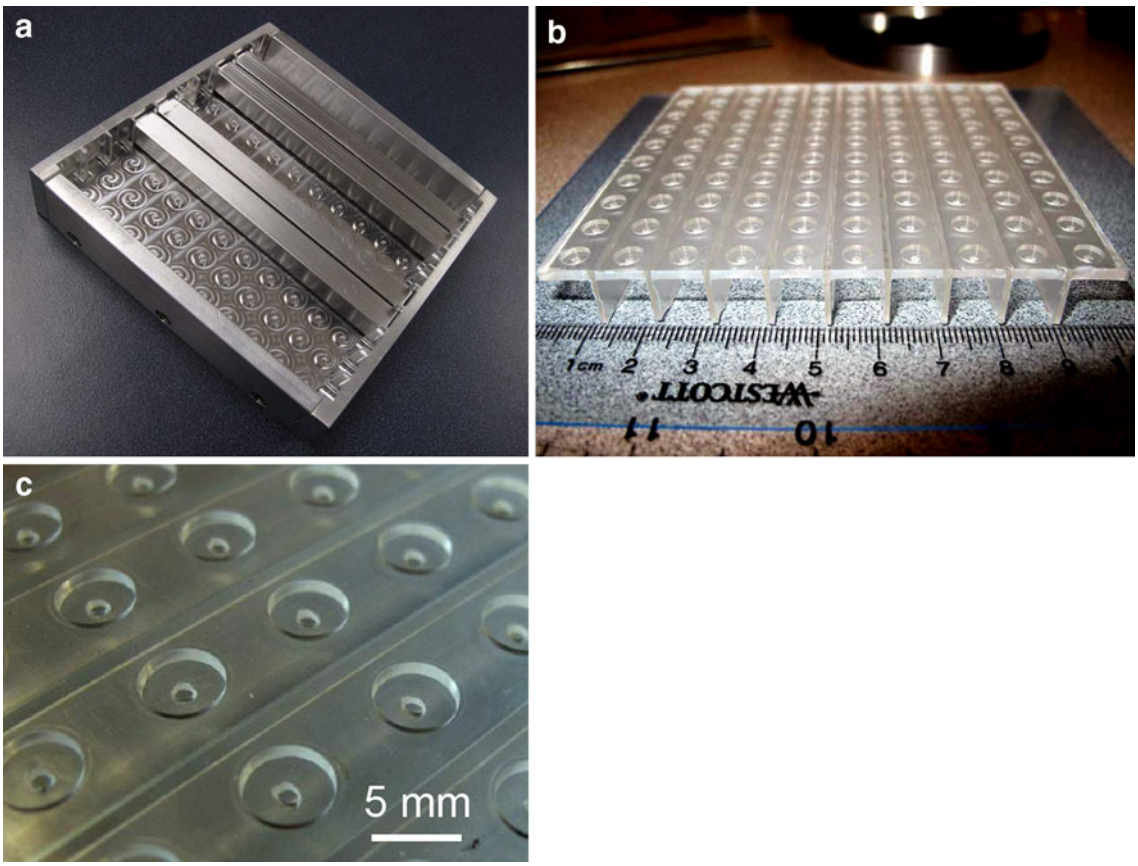

Fig. 5 Combination of synthetic jets and agitators by double-sided hot embossing. **a** CNC mold insert consisting of top and bottom molds on 10×10 cm^2 area. **b** Hot embossed polymer structures. **c** zoom-in synthetic jet array in (**b**)

Table 1 Hot embossing parameters

Process parameter	Value
Molding temperature	190°C
Molding force	20 ~ 30 kN on 10×10 cm^2 area
Molding time plus indentation	10 min
Demolding temperature	85°C

polymer was pressed into the mold cavity, and was redistributed during the molding process. The corners of the nozzles and the cavities are very sharp. This indicates that the polymer and the mold insert are completely in contact with the mold when at the viscous state. Figure 4 shows the hot-embossed, double-sided agitators. An assembly mold insert design ensures that all these high-aspect-ratio agitators are as designed after a demolding process. Figure 5 shows a hot-embossed, complex structure consisting of a synthetic jet array and agitators. A complete replication is achieved with no damage visible after the demolding process.

3.2 Confinement of viscous polymer flow

The deformability of polymers is improved when the molding state is shifted from a rubbery state to a viscous state. This will enhance the filling of a mold cavity with polymer. However, the requirement on pressure for directly filling a mold cannot be met by the squeezed flow, due to its low viscosity. This means that a viscous polymer still cannot fill the mold cavity itself without assistance. When a molding force is applied, the viscous polymer will flow into a free space instead of into a mold cavity. One possible solution is to increase the inner pressure driving the viscous flow by adding confinement of polymer viscous flow. We proposed two basic confinement configurations: (1) A metal ring was placed between a mold insert and a hot plate (Fig. 6a). The inner pressure was increased by squeezing the flow through a thin gap between the metal ring and the hot plate. This configuration runs well for a low-pressure requirement and small molding volume. The micro needle structure was completely replicated by this method. (2) The polymer was sealed by a mold insert, an outer chamber, and a piston (Fig. 6b). Higher inner pressure can be

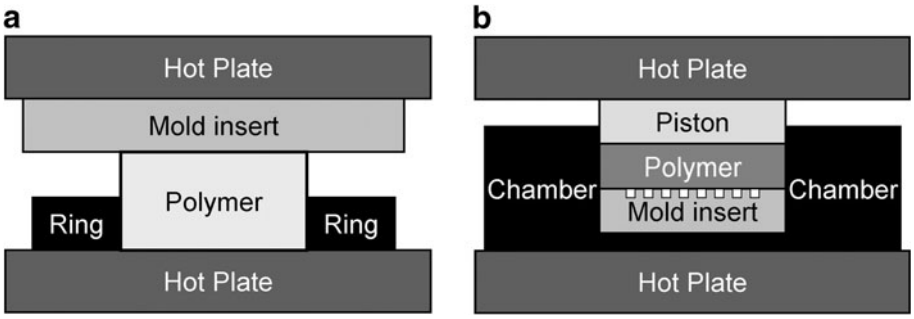

Fig. 6 Sketch of a confinement for polymer flow. **a** metal ring between a mold insert and a hot plate. **b** chamber and piston used to seal polymer

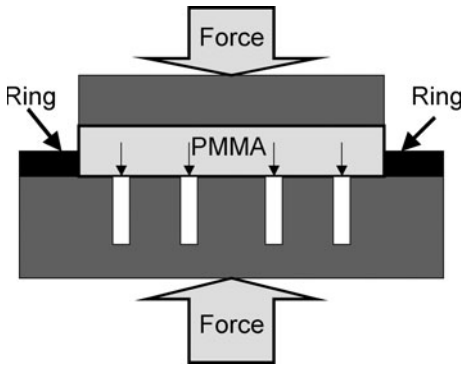

Fig. 7 Molded height dependency on molding process parameters

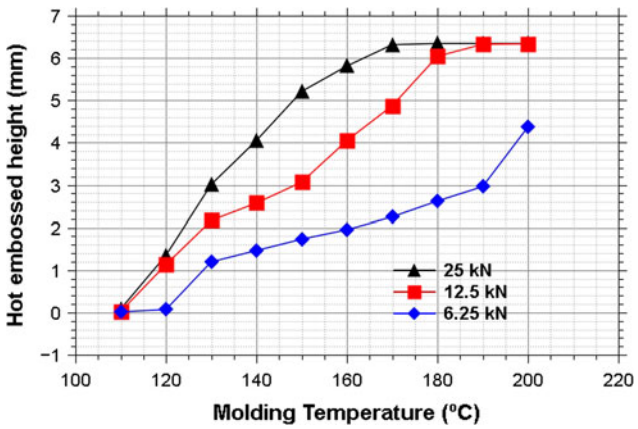

Fig. 8 Molded height dependency on molding temperature and force with confinement

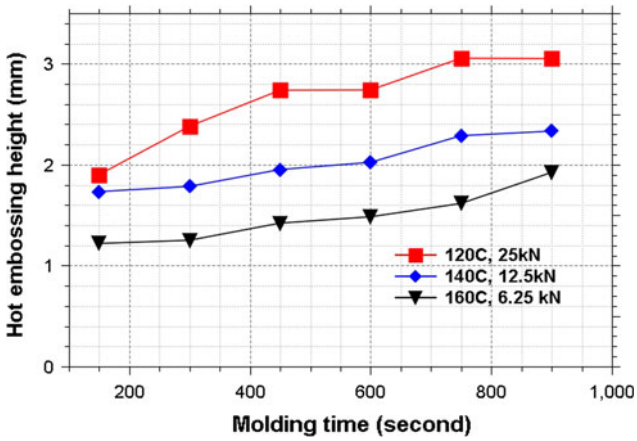

Fig. 9 Molded height dependency on molding time

achieved by a strong squeezed flow through a thin gap between the piston and the outer chamber. This configuration runs very well for a high-pressure requirement and a large molding volume. The millimeter-scale, complex polymer structures were completely replicated by this method.

3.3 Hot embossing process optimization

The hot embossing process is optimized by an investigation of the embossed feature height, molding temperature, force, and time. The experimental setup is shown in Fig. 7. The polymer sample of 4.5 mm thickness and 5 cm × 5 cm area was sandwiched between a hot plate and a mold insert. The molding force varied from 6.25 to 25 kN, with a molding temperature from 110 to 200°C. The molding time varied from 2.5 to 15 min. The molded height dependency on molding temperature and force is shown in Fig. 8. Molded height increases with molding temperature until it reaches a maximal height of 6.25 mm under sufficient molding force. Higher molding force of 25 kN allows a full molded height at a lower molding temperature of 170°C, or 190°C for a molding force of 12.5 kN. Even though a higher molding temperature causes better moldability, the polymer may become brittle after cooling from a higher temperature. Thus we select 190°C as the molding temperature.

Although the polymer deformability is increased for molding at a viscous state, the molding time still must be reconfigured for complex structures and large deformations. The molding time affects the molded height under various molding parameters, as shown in Fig. 9. This molded height dependency on molding time has almost the same trend for various molding parameters. The molded height increases with temperatures, and keeps relative stable after about 10 min. Although longer molding temperatures increase the molded height, this will cause the

molding process to have a low efficiency. Here, we select 10 min as typical molding time.

3.4 Polymer mass control

The total mass of polymer for hot embossing requires careful calculation to avoid waste of process time and raw material. The total mass of raw material, M_t, consists of two parts: embossed structure mass, M_e, and leakage mass, M_l. The leakage mass, M_l, will be squeezed through the gap. More leaking mass needs long molding time. Leakage mass can be reduced by applying less pressure, but this may negatively affect the molding process. A recommended balance between process time and raw materials is a leakage mass, M_l, of 5–10% of the embossed mass, M_e. The raw material may be in the form of multiple thin polymer sheets to match the total mass or thick PMMA sheets which match the total thickness. The former method is very flexible, but may cause air bubbles in the hot-embossed polymer. The latter requires careful machining to achieve the required thickness.

3.5 Thermal shrinkage of hot embossed polymer structures

The thermal shrinkage of hot embossed polymer structures is an important issue for process design, especially for large-size samples. In conventional hot embossing, thermal shrinkage of a polymer increases with the molding temperature, requiring a higher demolding force. Thus, lower molding temperatures are desired to reduce thermal shrinkage. Will thermal shrinkage increase observably for molding in the viscous state? We measured the whole structure thermal shrinkage after demolding. For a 102 mm (4 inch) PMMA hot embossed structure, thermal shrinkage is 0.6% on the side length. Although this shrinkage is comparable to molding at the rubbery state, the value cannot be ignored during the design of the mold insert and embossing process.

3.6 Processing time

The time of the embossing process we developed is higher than that in conventional hot embossing processes. Compared to hot embossing of thin polymer films, bulk embossing requires more heat and longer heating time. More molding time is also needed for a complex geometry. The normal molding time for micro hot embossing is several minutes, while the typical molding time is 10 min for our cases. More heating also requires longer cooling times.

The heating and cooling times can be decreased by more powerful heaters and stronger cooling systems. The molding process is still the most time consuming process step.

4 Conclusions

A novel hot embossing process by molding in the viscous state is presented in this paper. This method promises extreme polymer deformation due to low viscosity and high inner pressures, assisted by a confinement. Two types of confinements were proposed: a metal ring placed between a mold insert and a hot plate and an outer chamber with a piston to contain a mold insert and a polymer. Typical hot embossing process parameters were optimized; such as a molding temperature of 190°C with a molding force of 20 kN on a 10 cm × 10 cm area for a duration of 10 min. Various millimeter-scale polymer structures with a high aspect ratio and complex features were hot embossed. The typical microstructures were achieved by our developed hot embossing method. Compared with conventional hot embossing, this process consumes more time on the heating, molding, and cooling processes. However, it is acceptable for prototyping. Overall, this new approach promises some advantages, including excellent polymer deformability and compatibility with hot embossing processes.

Acknowledgments This work is sponsored by the DARPA MACE program, and partially carried out at the Nanofabrication Center at the University of Minnesota. We appreciate Mr. Dave Hultman's discussions on the design of mold inserts. The views expressed are those of the authors and do not reflect the official policy or position of the Department of Defense or the US Government. Approved for Public Release, Distribution Unlimited.

References

Chang HK, Kim YK (2000) UV-LIGA process for high aspect ratio structure using stress barrier and C-shaped etch hole. Sens Actuators A Phys 84:342–350. doi:10.1016/S0924-4247(00)00408-8

Choi C (2004) Fabrication of optical waveguides in thermosetting polymers using hot embossing. J Micromech Microeng 14:945–949. doi:10.1088/0960-1317/14/7/015

Chou SY, Krauss PR, Renstrom PJ (1995) Imprint of sub-25 nm vias and trenches in polymers. Appl Phys Lett 67:3114–3116. doi:10.1063/1.114851

Dittrich H (2004) Tool development for hot embossing of double-sided microstructured molded parts. Dissertation, University of Karlsruhe

Guo LJ (2004) Recent progress in nanoimprint technology and its applications. J Phys D Appl Phys 37:R123–R141. doi:10.1088/0022-3727/37/11/R01

Guo Y, Liu G, Xiong Y, Wang J, Huang X, Tian Y (2007) Study on hot embossing using Nickel and Ni-PTFE LIGA mold inserts. J MEMS 16:589–597. doi:10.1109/JMEMS.2007.896715

He Y, Fu JZ, Chen ZC (2007) Research on optimization of the hot embossing process. J Micromech Microeng 17:2420–2425. doi:10.1088/0960-1317/17/12/005

Heckele M, Schomburg WK (2004) Review on micro molding of thermoplastic polymers. J Micromech Microeng 14:R1–R14. doi:10.1088/0960-1317/14/3/R01

Heckele M, Bacher W, Muller KD (1998) Hot embossing—The molding technique for plastic microstructures. Microsyst Technol 4:122–124. doi:10.1007/s005420050112

Kumar G, Tang HX, Schroers J (2009) Nanomoulding with amorphous metals. Nature 457:868–873. doi:10.1038/nature07718

Mehne C, Steger R, Koltay P, Warkentin D, Heckele MP (2008) Large-area polymer microstructure replications through the hot embossing process using modular moulding tools. Proc Inst Mech Eng Part B J Eng Manuf 222:93–99. doi:10.1243/09544054JEM875

Pan CT, Su CH (2007) Fabrication of gapless triangular micro-lens array. Sens Actuators A 134:631–640. doi:10.1016/j.sna.2006.05.045

Roetting O, Kohler B, Reuther F, Blum H, Bacher W (1999) Production of movable metallic microstructures by aligned hot embossing and reactive ion etching. Proc SPIE 3680:1038–1045. doi:10.1117/12.341173

Shen XJ, Pan LW, Lin LW (2004) Microplastic embossing process: experimental and theoretical characterizations. Sens Actuators A 97–98:428–433. doi:10.1016/S0924-4247(02)00029-8

Taylor H, Lam YC, Boning D (2009) A computationally simple method for simulating the micro-embossing of thermoplastic layers. J Micromech Microeng 19:075007. doi:10.1088/0960-1317/19/7/075007

Ting CJ, Huang MC, Tsai HY, Chou CP, Fu CC (2008) Low cost fabrication of the large-area anti-reflection films from polymer by nanoimprint/hot-embossing technology. Nanotechnol 19:205301. doi:10.1088/0957-4484/19/20/205301

Worgull M (2009) Hot embossing—theory and technology of microreplication. William Andrew, Oxford, p 274

Worgull M, Heckele M, Schomburg WK (2005) Large-scale hot embossing. Microsyst Technol 12:110–115. doi:10.1007/s00542-005-0012-z

Worgull M, Hétu JF, Kabanemi KK, Heckele M (2006) Modeling and optimization of the hot embossing process for micro- and nanocomponent fabrication. Microsyst Technol 12:947–952. doi:10.1007/s00542-006-0124-0

Worgull M, Kolew A, Heilig M et al (2010) Hot embossing of high performance polymer. Microsys Technol. doi:10.1007/s00542-010-1155-0

Zhao Y, Cui T (2003) Fabrication of high-aspect-ratio polymer-based electrostatic comb drives using the hot embossing technique. J Micromech Microeng 13:430–435. doi:10.1088/0960-1317/13/3/312

Zhu X, Liu G, Xiong Y, Guo Y, Tian Y (2006) Fabrication of PMMA microchip of capillary electrophoresis by optimized UV-LIGA process. J Phys Conf Ser 34:875–879. doi:10.1088/1742-6596/34/1/145